

Quantum reflection and transmission of ballistic two-dimensional electrons by a potential barrier

X. Ying, J. P. Lu, J. J. Heremans, M. B. Santos, M. Shayegan, and S. A. Lyon
Department of Electrical Engineering, Princeton University, Princeton, New Jersey 08544

M. Littman

Department of Mechanical and Aerospace Engineering, Princeton University, Princeton, New Jersey 08544

P. Gross and H. Rabitz

Department of Chemistry, Princeton University, Princeton, New Jersey 08544

(Received 17 May 1994; accepted for publication 1 July 1994)

Measurements of the reflection and transmission coefficients of ballistic two-dimensional electrons by a potential barrier, induced via a surface gate, reveal that both coefficients vary *gradually* with the barrier height when it is less than the electron Fermi energy. Superimposed on the gradual variation, oscillatory structure which are consistent with interference resonances are also observed. The data imply that the potential barrier seen by the two-dimensional electrons is sharp compared to the electron wavelength.

The current trend of developing ever smaller solid-state electronic devices has placed them in the submicron regime where electron wave phenomena can no longer be neglected.¹ There is now the opportunity to conceive of and possibly realize novel devices that operate under entirely different principles from those used in conventional electronics. One such device, which encodes information directly on the electron wavepacket by passing the electrons over an array of potential wells and barriers, has been recently proposed.² In principle, such a device can be implemented in a low-disorder two-dimensional electron system (2DES) in a selectively doped GaAs/Al_xGa_{1-x}As heterojunction whose high mobility and hence long elastic mean-free path (typically $l_e \gg 1 \mu\text{m}$ at temperature ~ 1 K) ensures that the electron motion is ballistic and phase coherent (in 2DESs the phase coherence length $l_\phi > l_e$ at low temperatures). The potential barriers are induced by surface gate electrodes and adjusted individually by the corresponding gate voltage. A key requirement here is that the barrier edges be sharp compared to the electron Fermi wavelength, which is about 800 \AA for a 2DES of areal density $n = 10^{11}/\text{cm}^2$, in order to yield substantial internal quantum reflections in the barrier array and thus strong interference effects which are needed to shape the wavepacket.

Inducing sharp potential barriers with surface gate electrodes in a high-mobility 2DES is not a trivial issue. The 2DES is usually placed some distance away from the sample surface to achieve high mobilities by reducing scattering from remote ionized impurities. As a result, the potential barriers induced in such a system will be smooth because of the fringing fields. Although simple calculations of this effect are available,³ direct experimental measurements of the sharpness of the barriers in the complicated sample structure are needed. However, in most previous experiments, a potential barrier is used either as a boundary reflector when the barrier is above the electron Fermi energy E_f (e.g., to observe conductance fluctuations in a narrow channel,⁴ or magnetic focusing^{5,6}), or otherwise as a phase modulator⁷ or electron deflector.⁸ In the few experiments where the sharp-

ness of the barriers plays a role,⁹ the observed conductance fluctuations do not correspond to the expected resonance conditions and have been attributed to the inhomogeneities in the barriers because of the relatively strong disorder in the 2DES employed in the measurement.¹⁰ In this letter we report the measurement of the reflection and transmission coefficients (R and T) which vary smoothly as the height of a potential barrier is increased from zero until the transmission is cut off. In addition we observe interference resonances in R and T for the partially transmitting barrier. Our data clearly demonstrate that the potential barrier induced by a surface gate can indeed be sharp compared to the electron wavelength.

The GaAs/AlGaAs heterojunctions used in these measurements were grown by molecular beam epitaxy. The structure consists of a 42 nm Al_{0.38}Ga_{0.62}As spacer layer grown on top of a thick undoped GaAs layer, followed by ten δ -doped Si layers (with layer separation of 2 nm and Si density of $10^{12}/\text{cm}^2$ per layer), and a 6 nm GaAs cap layer. The 2DES is at 70 nm below the sample surface. To measure R and T , we fabricated a beam splitter structure on the sample surface by electron beam lithography as shown schematically in the inset to Fig. 1. It consists of an emitter (region 2), two collectors (regions 3 and 5), and a 0.2- μm -wide surface gate placed at 45° angle with respect to the electron beam from the emitter. The emitter and the collector regions were defined via shallow etched lines (the solid lines in Fig. 1 inset), and are connected to the central areas (regions 1 and 4) of the device via constrictions (point contacts) with a lithographic width of $\approx 1 \mu\text{m}$ and an estimated electrical channel width of $\approx 0.5 \mu\text{m}$ (when depletion is taken into account).⁶ Ohmic contacts to the regions 1–5 were made by alloying In in a H₂ ambient.

The sample was cooled down to 0.5 K in a ³He system. The 2DES has a density of $n = 1.7 \times 10^{11}/\text{cm}^2$ and a mobility $\mu = 1.2 \times 10^6 \text{ cm}^2/\text{V s}$, implying $l_e \approx 8 \mu\text{m}$ ($l_e = \hbar k_0 \mu / e$, where $k_0 = (2\pi n)^{1/2}$ is the electron wave vector). Ballistic transport is therefore dominant since the size of the beam splitter (about $6 \mu\text{m}$) is smaller than l_e . Standard, four-terminal, low

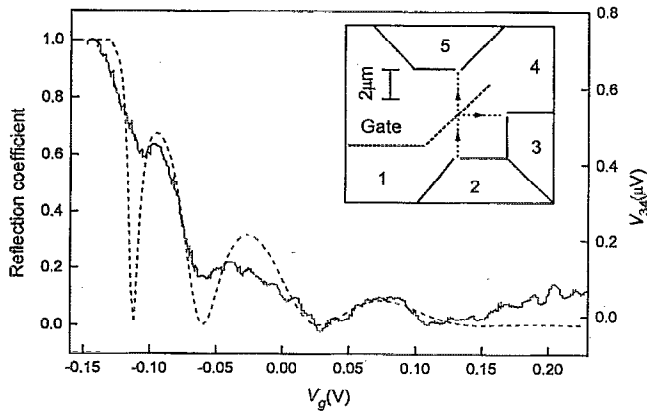


FIG. 1. Inset: schematic diagram of the beam splitter structure used in the measurement. The reflection coefficient measured as a function of gate voltage at $I_e=0.1 \mu\text{A}$ (solid curve). The dashed line is a fit to the data based on a square potential barrier model.

frequency ac techniques were used in the measurement. A fixed current (I_e) was applied between regions 1 and 2 (via corresponding ohmic contacts) to inject electrons from the emitter towards the potential barrier under the gate. As a measure of the number of electrons which are either reflected by or transmitted through the potential barrier, we recorded the voltages of regions 3 and 5 with respect to region 4, V_{34} (reflection) and V_{54} (transmission), as a function of the gate voltage V_g . Figure 1 shows V_{34} vs V_g for the device with $I_e=0.1 \mu\text{A}$. Note that this small emitter current ensures that the electron injection energy $E_e=eI_eR_{pc}$ (where R_{pc} is the emitter point contact resistance, typically 1–5 k Ω) is much smaller than $E_f(\cong 6.1 \text{ meV})$. We observed that V_{34} starts to saturate as $V_g < V_0 = -0.13 \text{ V}$ (see also Fig. 2). We associate V_0 with the onset of the threshold voltage for the barrier, i.e., the barrier is higher than E_f for $V_g < V_0$.¹¹ The reflection coefficient can therefore be normalized to the saturation value of V_{34} . As the barrier gets below E_f for $V_g > V_0$, R decreases gradually with the height of the potential barrier, or V_g . On top of this background, an oscillatory structure is also observed.

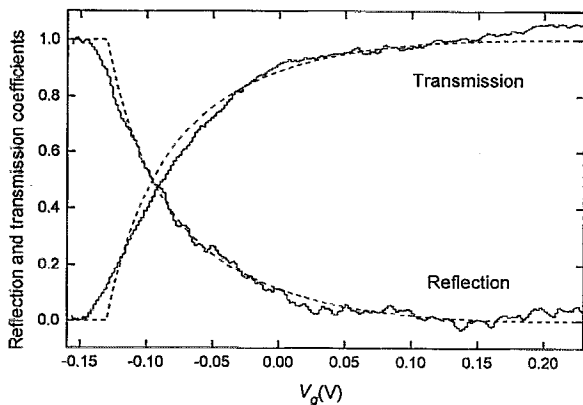


FIG. 2. Reflection and transmission coefficients measured as a function of gate voltage for a larger emitter current $I_e=1 \mu\text{A}$. The dashed curves are fits to the data based on a square potential barrier model (see text).

For a sharp (square) one-dimensional potential barrier, R and T can be easily derived from quantum mechanics:

$$T = \frac{1}{1 + 0.25(k/k_0 - k_0/k)^2 \sin^2(ka)}, \quad (1)$$

and $R=1-T$, where a is the width of the barrier, and k and k_0 are the wavevectors inside and outside the barrier region respectively. Two terms can be identified in Eq. (1). The term $(k/k_0 - k_0/k)^2$ leads to a monotonic background for R and T : R decreases from one to zero and T increases from zero to one, as k changes from zero to k_0 . The term $\sin^2(ka)$, which comes from the coherent interference of multiple reflections in the barrier, leads to oscillations in R and T on top of the monotonic background. Note that $R=0$ and $T=1$ whenever an integer number of electron half wavelengths fit in the barrier.

The data of Fig. 1 can be understood in terms of Eq. (1) if we associate k and k_0 with the component of the electron wave vector perpendicular to the barrier inside and outside the barrier region, respectively.¹² We have $k_0 = (2\pi n_0)^{1/2} \sin(45^\circ)$, where $n_0 = 1.7 \times 10^{11}/\text{cm}^2$ was measured with a Hall bar on the same device, and $k = c(V_g - V_0)^{1/2}$ if the electron density in the barrier varies linearly with V_g with a slope $\partial n/\partial V_g$. The dashed curve shown in Fig. 1 is a calculation of R for a square shape potential with c as a fitting parameter. The value of c from the fit suggests the effective $\partial n/\partial V_g$ for the 2DES under the narrow gate is a factor of 4 less than expected from the geometrical capacitance. In a sample from the same wafer and with a large gated area, we observed a similar (although somewhat smaller) discrepancy between $\partial n/\partial V_g$ and the value from the geometrical capacitance. We do not presently understand the origin of this discrepancy. The amplitude of the oscillation gets weaker near the threshold voltage ($k \rightarrow 0$), because l_ϕ and l_e of the 2DES under the gate decreases with decreasing density.

Some key features of the data were further examined through additional experiments. First, we checked the ballistic motion of electrons by applying a small magnetic field (B) perpendicular to the 2DES plane. For a totally reflecting barrier ($V_g < V_0$), the signal V_{34} at $B=0$ decreases as a finite B is applied in either polarity. This is expected: the applied B deflects the injected beam so that fewer electrons are reflected into the reflection-collector (region 3). For the polarity of B corresponding to the deflection of the injected electrons towards region 3, we observed the magnetic focusing effect.^{5,6} V_{34} shows strong oscillations as a function of B , and the B positions of the oscillation maxima are consistent with the density of the 2DES and the geometry of the structure. For the other polarity of B , we observed a monotonic decrease of V_{34} with increasing B , as expected.

Second, to check that the oscillatory structure in $R(V_g)$ originates from quantum interference, we increased the emitter current by a factor of 10 to $I_e=1 \mu\text{A}$. The corresponding electron injection energy $E_e \sim 1-5 \text{ meV}$ was then comparable to E_f . Yacoby *et al.* have demonstrated that at large injection energies, l_ϕ is greatly reduced due to electron-electron interactions and therefore the quantum interference effect is smeared out.⁷ Indeed, the oscillatory structures in our measured $R(V_g)$ nearly vanishes at the large emitter current as

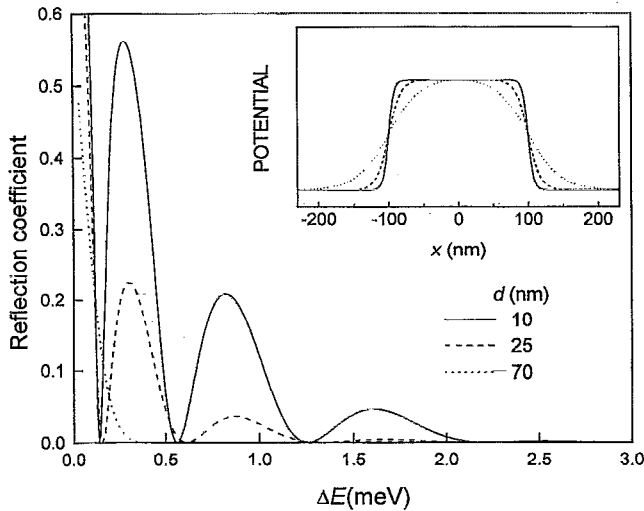


FIG. 3. Calculated reflection coefficients for the potential barriers whose normalized profiles, shown in the inset, are calculated for a square potential at the surface and represent the potential barriers seen by the 2DES which is at a distance d from the surface.

shown in Fig. 2 (also shown in the figure is T , deduced from V_{54} which was measured simultaneously with V_{34} ¹³). R and T can be well fitted by Eq. (1) (dashed curves) by simply substituting the oscillatory term in the equation with its average value, $\langle \sin^2(ka) \rangle = \frac{1}{2}$, while all the other parameters are the same as in Fig. 1.

The sharpness of the potential barrier deduced from the data of Figs. 1 and 2 is surprising. Although the exact shape of the potential barrier in the 2DES is not known, the fringing field effect can be estimated in a simple model where the Poisson equation is solved in the Fermi–Thomas screening approximation.^{3,14} In this model, the Fourier component of a surface potential barrier corresponding to the wavevector q decays with d as $\sim \exp(-qd)$, where d is the distance of the 2DES from the surface. Figure 3 shows the normalized potential barrier profile calculated for several d and the corresponding R for these barriers calculated as a function of $\Delta E = E_f - eV_b$, where V_b is the height of the potential barrier.¹⁴ Here we assumed $E_f = 3$ meV to account for the 45° orientation of the barrier with respect to the incident electron beam. The calculations suggest that R is very sensitive to the shape of the barrier. As d gets larger, the barrier gets smoother and the reflection is significantly reduced. For our sample ($d \approx 70$ nm), R is expected to be essentially zero except in the region where eV_b is very close to E_f ($\Delta E \approx 0$), in contrast to our measurements.

A comparison of Fig. 3 and the experimental data implies that the effective potential seen by the 2DES is sharper than expected from the simple model calculation. The origin of the apparent sharpness is not presently clear to us. It is tempting to consider the possibility that the sharpness may be related to the charging configuration of the ionized impurities in the dopant layers which are closer to the 2DES than the surface gate. If charging of the impurities with V_g takes place so that the effective electric field at the 2DES is partially screened, then both the potential sharpness and the experimental observation that $\partial n / \partial V_g$ is smaller than expected from the geometrical capacitance can be qualitatively explained. Future experiments and calculations to quantitatively understand R and T in such structures are planned.

The work was supported by the Army Research Office and the National Science Foundation.

- ¹ *Nanostructures and Mesoscopic Systems*, edited by W. P. Kirk and M. A. Read (Academic, New York, 1991).
- ² M. Littman, S. A. Lyon, H. Rabitz, and M. Shayegan (unpublished); P. Gross, V. Ramakrishna, E. Vilallonga, H. Rabitz, M. Littman, S. A. Lyon, and M. Shayegan, *Phys. Rev. B* **49**, 11100 (1994).
- ³ See, for example, P. J. Stiles, *Surf. Sci.* **73**, 252 (1978); S. E. Laux, D. J. Frank, and F. Stern, *Surf. Sci.* **196**, 101 (1988).
- ⁴ G. Timp, A. M. Chang, P. Mernkiewicz, R. Behringer, J. E. Cunningham, T. Y. Chang, and R. E. Howard, *Phys. Rev. Lett.* **59**, 732 (1987); K. Aihara, M. Yamamoto, and T. Mizutani, *Appl. Phys. Lett.* **63**, 3595 (1993), and references therein.
- ⁵ H. Van Houten, C. W. J. Beenakker, J. G. Williamson, M. E. I. Broekaart, P. H. M. van Loosdrecht, B. J. van Wees, J. E. Moozj, C. T. Foxon, and J. J. Harris *Phys. Rev. B* **39**, 8556 (1989).
- ⁶ J. J. Heremans, M. B. Santos, and M. Shayegan, *Appl. Phys. Lett.* **61**, 1652 (1992).
- ⁷ A. Yacoby, U. Sivan, C. P. Umbach, and J. M. Hong, *Phys. Rev. Lett.* **66**, 1938 (1991).
- ⁸ U. Sivan, M. Heiblum, C. P. Umbach, and H. Shtrikman, *Phys. Rev. B* **41**, 7937 (1990); J. Spector, H. L. Stormer, K. W. Baldwin, L. N. Pfeiffer, and K. W. West, *Appl. Phys. Lett.* **56**, 1290 (1990).
- ⁹ S. Washburn, A. B. Fowler, H. Schmid, and D. Kern, *Phys. Rev. B* **38**, 1554 (1988).
- ¹⁰ J. H. Davies and J. A. Nixon, *Phys. Rev. B* **39**, 3423 (1989).
- ¹¹ Because of the inhomogeneities in the potential barrier caused by the impurities, we do not expect a sharp threshold voltage (Ref. 10).
- ¹² In contrast to the experiment in Ref. 9, the wave vector direction of ballistic electrons in our device is well defined since the size of the corresponding point contacts is much smaller than the distance that the electrons travel and the reflection from the potential barrier is specular as verified in a separate experiment, although they were weaker than the oscillations in $R(V_g)$ data of Fig. 1.
- ¹³ Stronger oscillations were also observed in T at lower I_e . In general, the amplitude of the oscillations in R and T vs V_g were sample dependent, while the oscillation period and the monotonic backgrounds of R and T for the same device structure were not.
- ¹⁴ J. P. Lu, X. Ying, and M. Shayegan (unpublished).